

Enhanced Two-Photon Processes in Quantum Dots inside Photonic Crystal Nanocavities and Quantum Information Processing Applications

Ziliang Lin* and Jelena Vučković

E. L. Ginzton Laboratory, Stanford University, Stanford, California 94305, USA

(Dated: May 13, 2022)

Abstract

We show that the two-photon transition rates of quantum dots coupled to nanocavities are enhanced by up to 8 orders of magnitude relative to quantum dots in bulk host. We then propose how to take advantage of this enhancement to implement coherent quantum dot excitation by two-photon absorption, entangled photon pair generation by two-photon spontaneous emission, and single-photon generation at telecommunication wavelengths by two-photon stimulated and spontaneous emission.

INTRODUCTION

Recent progress in semiconductor quantum dots (QDs) coupled to photonic crystal (PC) cavities has shown that these coupled systems exhibit cavity quantum electrodynamics (QED) effects. Experiments have demonstrated creation of single photons in the near infrared[1, 2], Purcell enhancement of QD spontaneous emission rates in weak coupling regime[3, 4], polariton state splitting in strong coupling regime[5, 6], controlled amplitude and phase shifts at a single photon level[7], and photon induced tunneling and blockade[8]. These results indicate that the QDs can be combined with PCs in an integrated platform for quantum information science[9, 10, 11].

However, many important challenges remain in the QD-PC cavity systems. Among them is the generation of indistinguishable single photons, preferably at telecommunication wavelengths. The challenge of generating indistinguishable photons results from the fact that an incoherently excited QD has to undergo phonon assisted relaxation to the lowest excited state, so the single photons it emits have different temporal profiles[12, 13]. For this reason, the maximum demonstrated indistinguishability between photons emitted from a single QD has been around 82%[14]. This problem would be resolved by exciting QDs coherently inside the cavities. In addition, coherent excitation is of great interest for quantum information processing, as it also enables manipulation of QD states. However, this type of excitation experiments face the difficulty of separating signal and probe photons that have the same wavelength. Another challenge in the QD-PC cavity systems is the generation of entangled photon pairs[15]. Although photon pairs can be created from biexciton decay cascade in a QD[16, 17], the pairs are not entangled in polarization because the intermediate exciton states are split by anisotropic electron-hole exchange interactions[18, 19].

In this Letter, we analyze two-photon absorption (TPA) and emission (TPE) in QDs coupled to PC cavities as solutions to these challenges (Fig. 1). TPA allows coherent excitation of the QDs and at the same time the frequency separation of the signal and probe photons. TPA eliminates QD jitter when the frequencies of the two photons are tuned such that their sum matches the emission frequency of the QDs. On the other hand, TPE from an excited QD allows the generation of single photons and entangled photon pairs on demand at telecommunication wavelengths. We also show that semiconductor QDs coupled to PC cavities enable great enhancement of two-photon transition rates relative to slow rates in bulk host[20, 21, 22, 23].

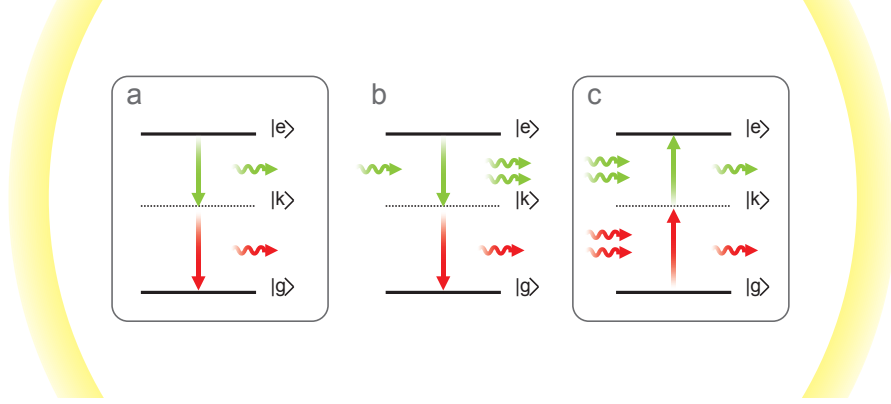


FIG. 1: (Color online) (a) Spontaneous emission of a pair of photons from an excited QD via a virtual state. (b) Stimulated TPE from an excited QD. The first photon emission is stimulated with an external laser and the second photon emission is spontaneous. (c) TPA by a QD. In all three processes, the transition rates are enhanced inside a single-mode or double-mode cavity (pictured here as a generic cavity) with frequencies matching the photon frequencies.

TRANSITION RATE CALCULATIONS AND DISCUSSION

Two-Photon Absorption and Emission by a QD in Bulk Semiconductor Host

We model the semiconductor QD as a two-level system with energy separation $\hbar(\omega_e - \omega_g) = \hbar\omega_d$, where \hbar is the reduced Planck's constant and ω_e (ω_g) is the excited (ground) state frequency (Fig. 1). The QD is illuminated by two laser beams of frequencies ω_1 and ω_2 . Assuming the QD is initially at its ground state, $c_g(t=0) = 1$, we first calculate the complex coefficient $c_k(t)$ for the k 'th virtual intermediate state with time-dependent perturbation theory,

$$c_k(t) = \frac{1}{i\hbar} \int_0^t \mathcal{V}_{gk}(t') e^{i(\omega_k - \omega_g)t'} c_g dt', \quad (1)$$

where

$$\mathcal{V}_{gk}(t) = \hbar\Omega_{gk,1} e^{-i\omega_1 t} + \hbar\Omega_{gk,2} e^{-i\omega_2 t} + \text{h.c.}, \quad (2)$$

and $\Omega_{gk,1}$ ($\Omega_{gk,2}$) is the Rabi transition rate between the ground state and the intermediate state driven by the laser with frequency ω_1 (ω_2). After calculating $c_e(t)$ from $c_k(t)$ with similar expressions, we obtain the nondegenerate two-photon transition rate from the ground state to the excited states,

$$\Gamma = 2\pi \left| \sum_k \left[\frac{\Omega_{gk,1}\Omega_{ke,2}}{\Delta_{gk,1}} + \frac{\Omega_{gk,2}\Omega_{ke,1}}{\Delta_{gk,2}} \right] \right|^2 \delta(\omega_d - \omega_1 - \omega_2), \quad (3)$$

where the summation is performed over all the virtual intermediate states. $\Delta_{gk,1}$ is the QD-light detuning $\omega_k - \omega_g - \omega_1$, and a similar expression holds for $\Delta_{gk,2}$. The delta function $\delta(\omega_d - \omega_1 - \omega_2)$ represents energy conservation. In degenerate two-photon transitions, $\omega_1 = \omega_2$ and the transition rate becomes

$$\Gamma = 2\pi \left| \sum_k \frac{\Omega_{gk,1} \Omega_{ke,1}}{\Delta_{gk,1}} \right|^2 \delta(\omega_d - 2\omega_1). \quad (4)$$

It must be pointed out that although Eqs. (3) and (4) are derived for TPA rates, TPE rate expressions hold the same form with $\Delta_{gk,1}$ ($\Delta_{gk,2}$) replaced by $\Delta_{ke,2}$ ($\Delta_{ke,1}$).

Cavity Enhanced Two-Photon Spontaneous Emission (TPSE)

Next we derive the nondegenerate TPSE rates for QD coupled to a PC cavity (Fig. 1a). We start from the expression for two-photon Rabi frequencies for an excited QD with quantized electric field:

$$\Omega_{gk,1} = \frac{\mathbf{d}_{gk} \cdot \mathbf{E}_1(\mathbf{r})}{\hbar} = \frac{|\mathbf{d}_{gk}|}{\hbar} \sqrt{\frac{(N_1 + 1)\hbar\omega_1}{2n^2\varepsilon_0 V_1}} \psi_{gk,1}, \quad (5)$$

where \mathbf{d}_{gk} is the transition dipole moment between the ground state and the intermediate state. $\mathbf{E}_1(\mathbf{r})$, N_1 , V_1 are respectively the electric field at the QD location, photon number, and the mode volume associated with the mode of frequency ω_1 that the QD is interacting with. n is the dielectric constant of the host substrate and ε_0 is the free space permittivity. $\psi_{gk,1}$ is a dimensionless number characterizing the reduction in Rabi rate due to position mismatch between the QD and the electric field maximum within the cavity.

$$\psi_{gk,1} = \frac{|\mathbf{E}_1(\mathbf{r})|}{|\mathbf{E}_1(\mathbf{r}_M)|} \left(\frac{\mathbf{d}_{gk} \cdot \mathbf{e}_1}{|\mathbf{d}_{gk}|} \right), \quad (6)$$

where $|\mathbf{E}_1(\mathbf{r}_M)|$ is the maximum field strength in the cavity, and \mathbf{e}_1 is the polarization of the field. Similar expressions hold for Rabi rates $\Omega_{ke,1}$, $\Omega_{gk,2}$, and $\Omega_{ke,2}$. Eqn. (3) then gives

$$\Gamma = 2\pi \frac{\omega_1 \omega_2 (N_1 + 1)(N_2 + 1)}{(2\hbar n^2 \varepsilon_0)^2 V_1 V_2} \left| \sum_k \left[\frac{|\mathbf{d}_{gk}| |\mathbf{d}_{ke}| \psi_{gk,1} \psi_{ke,2}}{\Delta_{gk,1}} + \frac{|\mathbf{d}_{gk}| |\mathbf{d}_{ke}| \psi_{gk,2} \psi_{ke,1}}{\Delta_{gk,2}} \right] \right|^2 \delta(\omega_d - \omega_1 - \omega_2). \quad (7)$$

To simplify our expression, we define

$$M_{12} = \left| \sum_k \left[\frac{|\mathbf{d}_{gk}| |\mathbf{d}_{ke}| \psi_{gk,1} \psi_{ke,2}}{\Delta_{gk,1}} + \frac{|\mathbf{d}_{gk}| |\mathbf{d}_{ke}| \psi_{gk,2} \psi_{ke,1}}{\Delta_{gk,2}} \right] \right|. \quad (8)$$

For TPSE rate, we need to integrate Eqn. (7) over all frequencies. By introducing $N(\omega_1) + 1 = \int d\omega_1 \rho_1(\omega_1)(\bar{N}(\omega_1) + 1)$, where $\rho_1(\omega_1)$ is the photon density of states and $\bar{N}(\omega_1)$ is the average photon number of frequency ω_1 , we obtain

$$\Gamma_{\text{tot}} = \frac{2\pi}{(2\hbar n^2 \varepsilon_0)^2 V_1 V_2} \int d\omega_1 d\omega_2 \omega_1 \omega_2 \rho_1(\omega_1) \rho_2(\omega_2) (\bar{N}(\omega_1) + 1) (\bar{N}(\omega_2) + 1) M_{12}^2 \delta(\omega_d - \omega_1 - \omega_2). \quad (9)$$

The expression is symmetric with respect to ω_1 and ω_2 and we are free to integrate over either variable. We integrate over $d\omega_1$ and set $\bar{N}(\omega_1) = \bar{N}(\omega_2) = 0$ for TPSE,

$$\frac{\partial \Gamma_{\text{tot}}}{\partial \omega_2} = \frac{2\pi}{(2\hbar n^2 \varepsilon_0)^2 V_1 V_2} \omega_1 \omega_2 \rho_1(\omega_1) \rho_2(\omega_2) M_{12}^2, \quad (10)$$

with energy conservation condition $\omega_1 + \omega_2 = \omega_d$.

We arrive at our final expression by writing explicitly the density of states $\rho(\omega)$. In bulk, $\rho(\omega_1) = V_1 n^3 \omega_1^2 / (3\pi^2 c^3)$ integrated over photon polarizations and dipole emission geometry. For a cavity $\omega_1 \rho(\omega_1) = 2Q_1 \phi_1 / \pi$, where Q_1 is the cavity quality factor and ϕ_1 is a dimensionless number characterizing frequency mismatch between ω_1 and cavity resonance frequencies ω_{1c} ,

$$\phi_1(\omega_1) = \frac{\omega_1 / \omega_{1c}}{1 + 4Q_1^2 (\omega_1 / \omega_{1c} - 1)^2}. \quad (11)$$

Finally, the two-photon emission rates for a QD in bulk semiconductor host ($\Gamma_0(\omega_1, \omega_2)$), in a single-mode cavity centered at ω_{1c} ($\Gamma_{\omega_{1c}}(\omega_1, \omega_2)$), and in a double-mode cavity centered at ω_{1c} and ω_{2c} ($\Gamma_{\omega_{1c}, \omega_{2c}}(\omega_1, \omega_2)$) are

$$\frac{\partial \Gamma_0}{\partial \omega_2} = \frac{\pi}{2} \left[\frac{n\omega_1^3}{3\pi \hbar \varepsilon_0 c^3} \right] \left[\frac{n\omega_2^3}{3\pi \hbar \varepsilon_0 c^3} \right] M_{12}^2 \text{ with all } \psi\text{'s} = 1, \quad (12a)$$

$$\frac{\partial \Gamma_{\omega_{1c}}}{\partial \omega_2} = \frac{\pi}{2} \left[\frac{2Q_1}{\hbar n^2 \varepsilon_0 V_1} \phi_1 \right] \left[\frac{n\omega_2^3}{3\pi \hbar \varepsilon_0 c^3} \right] M_{12}^2 \text{ with } \psi_{ke,2} = \psi_{gk,2} = 1, \text{ and} \quad (12b)$$

$$\frac{\partial \Gamma_{\omega_{1c}, \omega_{2c}}}{\partial \omega_2} = \frac{\pi}{2} \left[\frac{2Q_1}{\hbar n^2 \varepsilon_0 V_1} \phi_1 \right] \left[\frac{2Q_2}{\hbar n^2 \varepsilon_0 V_2} \phi_2 \right] M_{12}^2 \quad (12c)$$

with $\omega_1 + \omega_2 = \omega_d$.

Physically, TPSE occurs as the result of the interaction between the excited QD and the vacuum states of the electromagnetic field with modes frequencies ω_1 and ω_2 . Since there is a series of (ω_1, ω_2) satisfying the energy conservation condition $\omega_1 + \omega_2 = \omega_d$, the TPSE spectrum of a single QD is broad. Furthermore, the TPSE rate is slower than the one-photon emission because a series of virtual states are required for the TPSE. The combination of broad spectrum and low transition rate results in an overall low signal intensity, and therefore TPSE is generally difficult to detect.

However, the TPSE rate is enhanced when the QD is placed inside a cavity, because the cavity modifies the photon density of states in free space into a Lorentzian distribution (Eqn. (11)) and also localizes field into small volume V which leads to higher interaction strength. This rate enhancement is similar to the one-photon spontaneous emission rate enhancement, better known as the Purcell enhancement[24]. The two-photon rate enhancement relative to the bulk medium can be seen by taking the ratios of Eqs. (12b) and (12c) to Eqn. (12a). For single and double mode cavities, respectively:

$$\frac{\Gamma_{\omega_{1c}}}{\Gamma_0} = F_1 = \frac{3}{4\pi^2} \left(\frac{\lambda_1}{n}\right)^3 \frac{Q_1}{V_1} \phi_1 \quad \text{and} \quad (13a)$$

$$\frac{\Gamma_{\omega_{1c}, \omega_{2c}}}{\Gamma_0} = F_1 F_2 = \left[\frac{3}{4\pi^2} \left(\frac{\lambda_1}{n}\right)^3 \frac{Q_1}{V_1} \phi_1 \right] \left[\frac{3}{4\pi^2} \left(\frac{\lambda_2}{n}\right)^3 \frac{Q_2}{V_2} \phi_2 \right], \quad (13b)$$

where F_1 (F_2) is the Purcell factor for frequency ω_1 (ω_2), and λ_1 (λ_2) is the free-space wavelength for the corresponding frequency. Clearly, a double-mode cavity gives a greater rate enhancement than a single-mode cavity, as expected.

Therefore, the two-photon emission rate from a QD can be greatly enhanced in a cavity. Experimentally, single-mode cavities with Q 's exceeding 10^4 and mode volumes below cubic optical wavelength have been demonstrated, and doubly resonant cavities with similar Q 's and mode volumes have been proposed[25]. Therefore, we expect the QD TPSE to be increased by up to 4 orders of magnitude in single-mode cavities and by 8 orders of magnitude in double-mode cavities. Second, in photonic crystal cavities only the emission rates with frequency pair (ω_1, ω_2) matching the cavity frequencies $(\omega_{1c}, \omega_{2c})$ are enhanced while emission rates with other frequency pairs are greatly suppressed as a result of the reduction in photon density of states relative to the bulk medium. Thus, the cavities offer good controls over the frequencies of emitted photons. Third, inside a double-mode cavity with degenerate polarizations for both modes, the two emitted photons are entangled in polarization.

Cavity Enhanced Two-Photon Absorption

For QD TPA when it is coupled to the cavity (Fig. 1c), the Rabi rate takes the form of

$$\Omega_{gk,1} = \frac{|\mathbf{d}_{gk}|}{\hbar} \left[\frac{N_1 \hbar \omega_1}{2n^2 \varepsilon_0 V_1} \right]^{1/2} \psi_{gk,1} = \frac{|\mathbf{d}_{gk}|}{\hbar} \left[\frac{\eta_1 P_1 Q_1}{\pi n^2 \varepsilon_0 V_1 \omega_1} \phi_1 \right]^{1/2} \psi_{gk,1}. \quad (14)$$

where P_1 and η_1 are respectively the laser power and coupling efficiency into the cavity. When the QD is not coupled to the cavity, $2n\varepsilon_0c|\mathbf{E}_1|^2A_1 = P_1$ and the Rabi rate is

$$\Omega_{gk,1} = \frac{|\mathbf{d}_{gk}|}{\hbar} \left[\frac{P_1}{2n\varepsilon_0cA_1} \right]^{1/2} \psi_{gk,1}. \quad (15)$$

where A_1 is the laser beam spot radius. The TPA rates are then

$$\begin{aligned} \Gamma_0 &= \frac{\pi}{2} \left[\frac{P_1}{2\hbar^2n\varepsilon_0cA_1} \right] \left[\frac{P_2}{2\hbar^2n\varepsilon_0cA_2} \right] M_{12}^2 \delta(\omega_d - \omega_1 - \omega_2), \\ \Gamma_{\omega_{1c}} &= \frac{\pi}{2} \left[\frac{\eta_1 P_1 Q_1}{\pi \hbar^2 \omega_1 n^2 \varepsilon_0 V_1} \phi_1 \right] \left[\frac{P_2}{2\hbar^2 n \varepsilon_0 c A_2} \right] M_{12}^2 \delta(\omega_d - \omega_1 - \omega_2), \text{ and} \\ \Gamma_{\omega_{1c}, \omega_{2c}} &= \frac{\pi}{2} \left[\frac{\eta_1 P_1 Q_1}{\pi \hbar^2 \omega_1 n^2 \varepsilon_0 V_1} \phi_1 \right] \left[\frac{\eta_2 P_2 Q_2}{\pi \hbar^2 \omega_2 n^2 \varepsilon_0 V_2} \phi_2 \right] M_{12}^2 \delta(\omega_d - \omega_1 - \omega_2). \end{aligned} \quad (16)$$

In the nondegenerate TPA, the absorption rate has a linear dependence on P_1 and P_2 ; in the degenerate case, the absorption rate has a quadratic dependence on P_1 .

Similar to the TPSE rate, the TPA rate is enhanced because the cavity modifies the photon density of states. For the same excitation laser power, the rate enhancement is

$$\begin{aligned} \frac{\Gamma_{\omega_{1c}}}{\Gamma_0} &= \frac{2\eta_1 Q_1}{\pi} \frac{A_1 \lambda_1}{V_1 n}, \text{ and} \\ \frac{\Gamma_{\omega_{1c}, \omega_{2c}}}{\Gamma_0} &= \left[\frac{2\eta_1 Q_1}{\pi} \frac{A_1 \lambda_1}{V_1 n} \right] \left[\frac{2\eta_2 Q_2}{\pi} \frac{A_2 \lambda_2}{V_2 n} \right]. \end{aligned} \quad (17)$$

Two-photon excitation of QDs holds several advantages over conventional one-photon excitation. By tuning ω_1 and ω_2 to match $\omega_1 + \omega_2 = \omega_d$, we can coherently excite a QD and therefore create a source of indistinguishable single photons on demand. This is because we eliminate a 10-30 ps time jitter in emitted single photons resulting from incoherent excitation of a QD to a higher energy state from which a phonon-assisted relaxation to the first excited state happens[12]. Two-photon excitation presents a solution to the separation of signal and probe photons, because the excitation and emission wavelengths are different. Finally, TPA offers a convenient tool to coherently excite and manipulate a QD, which is of interest for quantum information processing[26].

Cavity Enhanced Two-Photon Stimulated Emission (TPSTE)

With similar calculations, we derive the TPSTE rate in a double-mode cavity with stimulation by a laser beam with power P_2 and frequency ω_2 , whose coupling efficiency to the cavity mode is denoted as η_2 ,

$$\Gamma_{\omega_{1c}, \omega_{2c}} = \frac{\pi}{2} \left[\frac{2Q_1}{\pi \hbar n^2 \varepsilon_0 V_1} \phi_1 \right] \left[\frac{\eta_2 P_2 Q_2}{\hbar^2 \omega_2 n^2 \varepsilon_0 V_2} \phi_2 \right] M_{12}^2. \quad (18)$$

The excited QD is stimulated with either ω_1 or ω_2 -frequency light and spontaneously emits single photons of the complementary frequency. Fig. 1b shows the stimulation emission of a photon of frequency ω_2 and the spontaneous emission of a photon of frequency ω_1 . Eqs. (18) and (12c) show that the TPSTE rate is linearly dependent on the stimulation light power and the rate is increased by a factor of $\eta_2 P_2 / (2\pi\hbar\omega_2)$ comparing with the TPSE rate. This additional enhancement makes the QD an selective single photon emitter at λ_1 .

EXPERIMENTAL PROPOSAL AND QUANTUM INFORMATION PROCESSING APPLICATIONS

We propose to experimentally demonstrate enhanced two-photon absorption and emission in InAs QDs embedded in two-dimensional GaAs double-mode PC cavities (Fig. 2a). Since the QDs have ground and excited state splitting ranging from 900 nm to 950 nm, we select two photon frequencies as $\lambda_1 = 1550$ nm and $\lambda_2 = 2300$ nm, conveniently coinciding with the telecommunication band (suitable for propagation down the fiber) and emission from existing GaSb lasers, respectively. To generate indistinguishable single photons on demand, we excite a QD with TPA and collect single photons emitted at $\lambda_d = 926$ nm (Fig. 2d). This resonant excitation eliminates jitter completely, thereby leading to indistinguishable single photons. To generate entangled photon pairs, we excite a QD with one-photon absorption and collect photon pairs at (1550, 2300) nm via TPSE (Fig. 2e). In addition, when we stimulate this excited QD with a 2300 nm laser beam, we can generate 1550 nm photons on demand.

An examination of Eqn. (8) reveals that two-photon transitions have an opposite parity selection rules than one-photon transitions. In an one-photon transition, the ground and excited states need to have opposite parity so that the transition dipole moment $|\mathbf{d}_{ge}|$ is nonzero. On the other hand, a two-photon transition requires the ground and excited states having the same parity for $|\mathbf{d}_{gk}||\mathbf{d}_{ke}|$ to be nonzero. This selection rule discrepancy implies that two-photon transitions cannot connect states that have one-photon transitions and vice versa. For a QD in the effective mass approximation, its energy eigenfunctions can be written as a product of an periodic function $u(\mathbf{r})$ and an envelope function $f(\mathbf{r})$, where $f(\mathbf{r})$ satisfies the Schrödinger equation with effective mass. Since $u(\mathbf{r})$ has even parity for the valence band states but odd parity for the conduction band states, an interband one-photon transition is allowed when its initial and final state envelop functions have the same parity (i.e. s shell- s shell and p shell- p shell transitions, as shown in Fig. 2b)[28], while

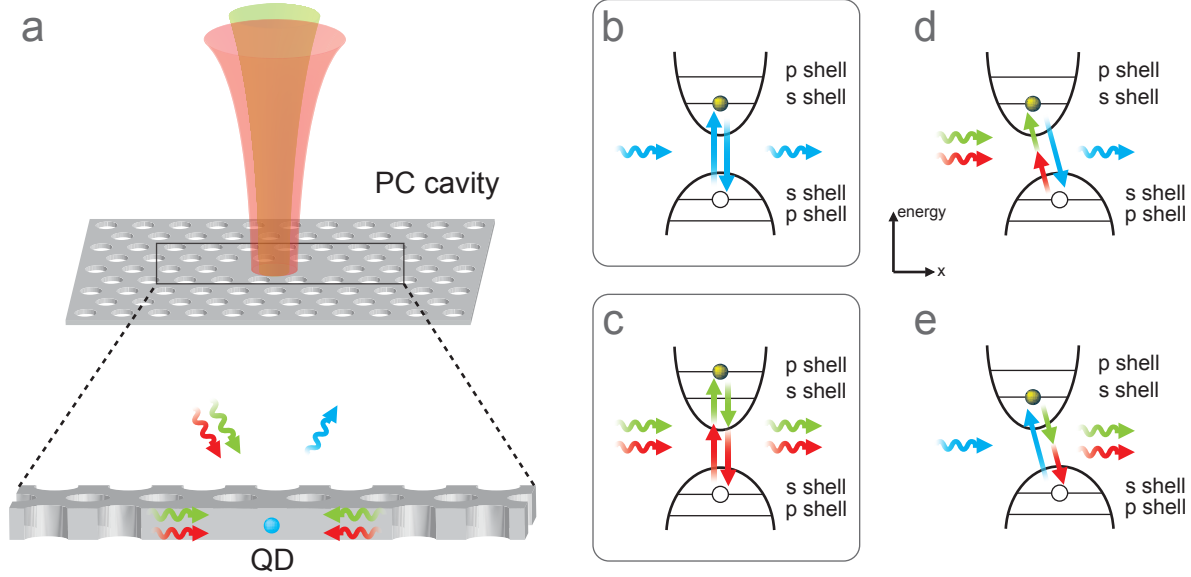


FIG. 2: (Color online) (a) Setup for enhanced two-photon absorption experiment: two laser beams with frequencies ω_1 and ω_2 are injected to a double-mode cavity. (b) and (c) Parity selection rules dictate that one-photon valence band *s* shell to conduction band *s* shell absorption and emission are allowed but two-photon *s* shell-*s* shell absorption and emission are forbidden. However, two-photon *s* shell-*p* shell absorption and emission are permitted. The *p* shell is approximately 10 meV above the *s* shell in InAs QDs[27]. (d) Enhanced two-photon absorption and single-photon generation in a QD with a DC lateral electric field applied to it along the *x* direction. The lateral electric field shifts apart the hole valence band and the electron conduction band and therefore breaks the parity selection rule. DC field could be turned off in this step to enhance the one photon transition rate. The electron is first excited to the *s* shell in the conduction band via two-photon absorption, leaving a heavy hole in the *s* shell in valence band. The electron then recombines with the hole and generates a single photon. For a particular choice of the applied field, both one and two photon *s* shell- *s* shell transitions are permitted (Fig. 3). Alternatively, DC field could be turned off in this step to enhance the one photon transition rate in (b). (e) Enhanced two-photon spontaneous emission in a QD as a reverse process of two-photon absorption. The one-photon excited electron recombines with the hole and generates entangle photon pairs at (1550, 2300) nm via two-photon spontaneous emission.

an interband two-photon transitions is allowed when its initial and final state envelope functions have the opposite parity (i.e. *s* shell-*p* shell transition and vice versa, as shown in Fig. 2c).

To solve this problem, we propose the application of lateral electric fields to break the parity symmetry in wavefunctions. Recent experiments have demonstrated the Stark shift of QD

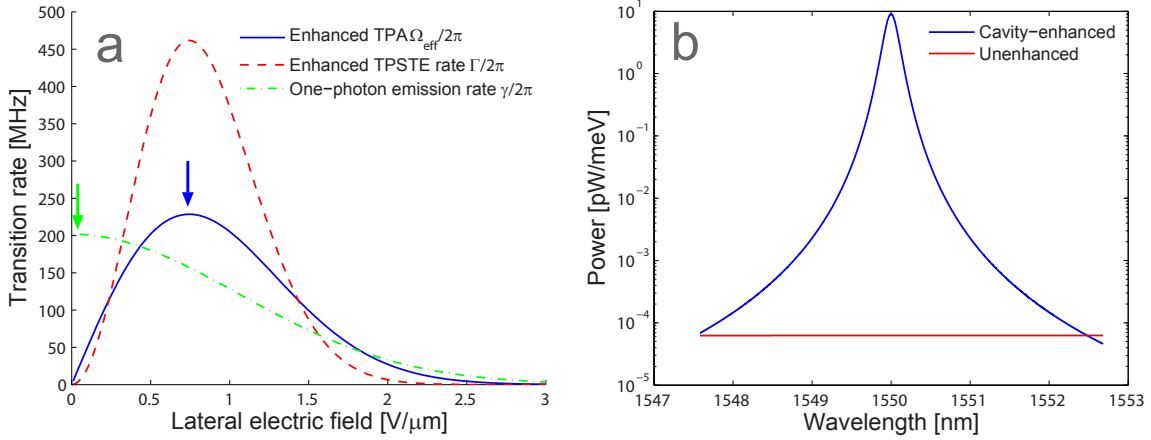


FIG. 3: (Color online) (a) Cavity-enhanced two-photon absorption effective Rabi rate (blue solid line), enhanced two-photon stimulated emission rate (red dashed line), and one-photon spontaneous emission rate (green dash-dot line) as a function of lateral electric field strength. All of the transitions are s shell- s shell. The simulation parameters are shown in text. (b) Cavity-enhanced two-photon spontaneous emission power (blue) and unenhanced emission power (red) of 1550 nm photons. Pairs of photons of 1550 nm and 2300 nm wavelength are emitted from the excited QD.

transitions[29, 30]. Following Korkusinski and Reimer *et al.* in Ref. [31] and [29], we model the QD as a particle in a finite well along its growth axis and a two-dimensional simple harmonic oscillator perpendicular to its growth axis. Denote the electron (hole) effective mass and oscillator frequency as m_e^* and ω_e (m_h^* and ω_h). For the one-photon s shell- s shell transition, the lateral electric field \mathcal{E} reduces its s shell- s shell transition dipole moment with expression $\mathbf{d}_{ge} = e\mathbf{r}_{cv} \exp[-(\Delta x)^2/(4l_e^2)]$, where $\mathbf{r}_{cv} = \int_V d\mathbf{r} u_c(\mathbf{r})\mathbf{r}u_v(\mathbf{r})$ is the transition moment between the valence band and the conduction band integrated over an unit cell, $\Delta x = e\mathcal{E}[(m_e^*\omega_e^2)^{-1} + (m_h^*\omega_h^2)^{-1}]$ is the separation of the electron and hole wavefunction centers, and $l_e = l_h = \sqrt{\hbar/(2m_e^*\omega_e)}$ is the oscillator length. For the two-photon s shell- s shell transition, the predominant intermediate states are the conduction and valence p shell states. The product of transition moment is calculated to be $|\mathbf{d}_{gk}||\mathbf{d}_{ke}| = e^2|\mathbf{r}_{cv}|\Delta x \exp[-(\Delta x)^2/(4l_e^2)]$ for both intermediate states.

Fig. 3a shows the enhanced TPA effective Rabi rate $\Omega_{\text{eff}} \equiv \Omega_{gk,1}\Omega_{ke,2}/\Delta_{gk,1}$, enhanced TPSE rate, and one-photon spontaneous emission rate as a function of lateral electric field. The simulation parameters are $m_h^* = 2m_e^* = 0.11m_0$ (m_0 is the electron rest mass), $\hbar\omega_e = 2\hbar\omega_h = 12$ meV[31], $|\mathbf{r}_{cv}| = 0.6$ nm[32], $\eta_1 = \eta_2 = 2\%$, $Q_1 = Q_2 = 5000$, $V_1 = (\lambda_1/n)^3$, $V_2 = (\lambda_2/n)^3$,

ϕ 's= 1, and ψ 's= 1. $P_1 = P_2 = 12 \mu\text{W}$ for enhanced TPA and $P_2 = 100 \mu\text{W}$ for enhanced TPSTE. The assumed low incoupling efficiencies of 2% are taken from the cavity QED experiments where the input laser beam is coupled to the cavity in the direction perpendicular to the chip[6, 7, 8]. However, It must be pointed out that the power required is even lower when the light is more efficiently coupled into the PC cavity. For example, PC cavities coupled to fiber tapers or PC waveguide can achieve a coupling efficiency of 70-90%[33, 34]. For enhanced TPA and subsequent single photon generation (Fig. 2d), we operate in the region where $\mathcal{E} < 0.5 \text{ V}/\mu\text{m}$ with $\Omega_{\text{eff}}/2\pi < \gamma/2\pi$ ($\gamma/2\pi$ is the one-photon spontaneous emission rate) to prevent Rabi oscillations between the ground and excited states. The electric field of $1 \text{ V}/\mu\text{m}$ strength only shifts the s shell- s shell transition by approximately 0.1 nm [29], therefore the QD is still on resonance with the double-mode cavity. In the case that the cavity also possesses a resonance mode at 926 nm , the single photon generation rate will be further enhanced by the Purcell factor at this mode. For enhanced TPSTE in 1550 nm -photon generation, we operate in the region such that $\Gamma > \gamma/2\pi$ to prevent 926 nm one-photon spontaneous emission of the excited QD. This implies that $\mathcal{E} > 0.3 \text{ V}/\mu\text{m}$. Fig. 3b shows the power of 1550 nm photons emitted by enhanced TPSE. The figure shows that the peak power of a single QD is on the same order as the power from a $200\text{-}\mu\text{m}$ -thick GaAs sample with carrier concentration of $1.2 \times 10^{18} \text{ cm}^{-3}$ [23].

In addition to the application of a static electric field, a modulation of electric field can change the parity selection rules dynamically. For example, we keep the electric field on at approximately $0.75 \text{ V}/\mu\text{m}$ to enable the s shell- s shell excitation via TPA (Fig. 3a blue arrow), but then turn off the field to permit a rapid single photon emission (Fig. 3a green arrow). This way we can permit both an efficient excitation and an efficient photon emission, because this approach allows for maximum transition rates in both steps. For an estimation of the modulation speed, we need to switch the electric field on a timescale that is faster than the recombination rate for an excited QD, which is 100 ps - 1 ns . Today's commercial function generators can easily achieve this speed.

CONCLUSION

We have derived the expressions for enhancement of two-photon spontaneous emission, two-photon stimulated emission, and two-photon absorption from a single QD in an optical nanocavity. Up to 8 orders of magnitude in rate enhancement is possible. We have also discussed how this could be applied to several important challenges in quantum information processing. In par-

ticular, Purcell enhanced two-photon spontaneous emission generates entangled photon pairs in polarization; enhanced two-photon stimulated emission further increases the emission rate and allows single photon generation at telecommunication wavelengths; enhanced two-photon absorption allows coherent excitation of quantum dots and eliminates jitter, thus enabling generation of indistinguishable single photons on demand.

Although we use semiconductor QDs as an illustration for cavity enhanced TPA and TPE in this paper, we can excite and manipulate other emitters such as 637 nm nitrogen-vacancy centers by laser beams in the 1550 nm telecommunication range. The cavity enhanced TPA and TPE can even enable construction of hybrid quantum networks containing different emitters just by changing the frequency of one of the excitation lasers.

The authors gratefully acknowledge financial support provided by National Science Foundation and the Army Research Office. Z. L. was supported by the NSF Graduate Fellowship and Stanford Graduate Fellowship.

* Electronic address: carterlin@stanford.edu

- [1] D. Englund, A. Faraon, B. Zhang, Y. Yamamoto, and J. Vuckovic, *Opt. Express* **15**, 5550 (2007).
- [2] S. Laurent, S. Varoutsis, L. L. Gratiet, A. Lematre, I. Sagnes, F. Raineri, A. Levenson, I. Robert-Philip, and I. Abram, *Appl. Phys. Lett.* **87**, 163107 (2005).
- [3] D. Englund, D. Fattal, E. Waks, G. Solomon, B. Zhang, T. Nakaoka, Y. Arakawa, Y. Yamamoto, and J. Vuckovic, *Phys. Rev. Lett.* **95**, 013904 (2005).
- [4] K. Hennessy, A. Badolato, M. Winger, D. Gerace, M. Atature, S. Gulde, S. Falt, E. L. Hu, and A. Imamoglu, *Nature* **445**, 896 (2007).
- [5] T. Yoshie, A. Scherer, J. Hendrickson, G. Khitrova, H. M. Gibbs, G. Rupper, C. Ell, O. B. Shchekin, and D. G. Deppe, *Phys. Rev. Lett.* **432**, 200 (2004).
- [6] D. Englund, A. Faraon, I. Fushman, N. Stoltz, P. Petroff, and J. Vuckovic, *Nature* **450**, 857 (2007).
- [7] I. Fushman, D. Englund, A. Faraon, N. Stoltz, P. Petroff, and J. Vuckovic, *Science* **320**, 769 (2008).
- [8] A. Faraon, I. Fushman, D. Englund, N. Stoltz, P. Petroff, and J. Vuckovic, *Nat. Phys.* **4**, 859 (2008).
- [9] J. I. Cirac, P. Zoller, H. J. Kimble, and H. Mabuchi, *Phys. Rev. Lett.* **78**, 3221 (1997).
- [10] L.-M. Duan, M. D. Lukin, J. I. Cirac, and P. Zoller, *Nature* **414**, 413 (2001).
- [11] L.-M. Duan and H. J. Kimble, *Phys. Rev. Lett.* **92**, 127902 (2004).

- [12] J. Vuckovic, D. Englund, D. Fattal, E. Waks, and Y. Yamamoto, *Physica E* **2**, 466 (2006).
- [13] C. Becher, A. Kiraz, P. Michler, W. V. Schoenfeld, P. M. Petroff, L. Zhang, E. Hu, and A. Imamoglu, *Physica E* **13**, 412 (2002).
- [14] C. Santori, D. Fattal, J. Vuckovic, G. S. Solomon, and Y. Yamamoto, *Nature* **419**, 594 (2002).
- [15] O. Benson, C. Santori, M. Pelton, and Y. Yamamoto, *Phys. Rev. Lett.* **84**, 2513 (2000).
- [16] N. Akopian, N. H. Lindner, E. Poem, Y. Berlatzky, J. Avron, D. Gershoni, B. D. Gerardot, and P. M. Petroff, *Phys. Rev. Lett.* **96**, 130501 (2006).
- [17] R. M. Stevenson, R. J. Young, P. Atkinson, K. Cooper, D. A. Ritchie, and A. J. Shields, *Nat. Phys.* **439**, 179 (2005).
- [18] D. Gammon, E. S. Snow, B. V. Shanabrook, D. S. Katzer, and D. Park, *Phys. Rev. Lett.* **76**, 3005 (1996).
- [19] M. Bayer, G. Ortner, O. Stern, A. Kuther, A. A. Gorbunov, A. Forchel, P. Hawrylak, S. Fafard, K. Hinzer, T. L. Reinecke, et al., *Phys. Rev. B* **65**, 195315 (2002).
- [20] A. F. Jarjour, T. J. Parker, R. A. Taylor, R. W. Martin, and I. M. Watson, *Phys. Status Solidi (C)* **2**, 3843 (2005).
- [21] L. A. Padilha, J. Fu, D. J. Hagan, E. W. V. Stryland, C. L. Cesar, L. C. Barbosa, C. H. B. Cruz, D. Buso, and A. Martucci, *Phys. Rev. B* **75**, 075325 (2007).
- [22] G. Xing, W. Ji, Y. Zheng, and J. Y. Ying, *Appl. Phys. Lett.* **93**, 241114 (2008).
- [23] A. Hayat, P. Ginzburg, and M. Orenstein, *Nat. Photonics* **2**, 238 (2008).
- [24] E. M. Purcell, *Phys. Rev.* **69**, 674 (1946).
- [25] J. Vuckovic, M. Loncar, H. Mabuchi, and A. Scherer, *Phys. Rev. E* **65**, 016608 (2001).
- [26] D. Englund, A. Majumdar, A. Faraon, M. Toishi, N. Stoltz, P. Petroff, and J. Vuckovic, Submitted to *Nature* (2009), arXiv:0902.2428v2.
- [27] P. Michler, *Single Quantum Dots: Fundamentals, Applications and New Concepts* (Springer, 2003).
- [28] P. Michler, *Single quantum dots: fundamentals, applications, and new concepts* (Springer, 2003).
- [29] M. E. Reimer, M. Korkusinski, D. Dalacu, J. Lefebvre, J. Lapointe, P. J. Poole, G. C. Aers, W. R. McKinnon, P. Hawrylak, and R. L. Williams, *Phys. Rev. B* **78**, 195301 (2008).
- [30] A. Laucht, F. Hofbauer, N. Hauke, J. Angele, S. Stobbe, M. Kaniber, G. Bohm, P. Lodahl, M.-C. Amann, and J. J. Finley, *New J. Phys.* **11**, 023034 (2009).
- [31] M. Korkusinski, M. E. Reimer, R. L. Williams, and P. Hawrylak, *Phys. Rev. B* **79**, 035309 (2009).
- [32] P. G. Eliseev, H. Li, A. Stintz, G. T. Liu, T. C. Newell, K. J. Malloy, and L. F. Lester, *Appl. Phys. Lett.*

77, 262 (2000).

[33] I.-K. Hwang, S.-K. Kim, J.-K. Yang, S.-H. Kim, S. H. Lee, and Y.-H. Lee, Appl. Phys. Lett. **87**, 131107 (2005).

[34] A. Faraon, E. Waks, D. Englund, I. Fushman, and J. Vuckovic, Appl. Phys. Lett. **90**, 073102 (2007).